Environmental Science & Technology

pubs.acs.org/est

Article

Oxidative Dissolution of Sulfide Minerals Tends to Accumulate More Dissolved Heavy Metals in Deep Seawater Environments than in Shallow Seawater Environments

Siyi Hu, Chunhui Tao,* Shili Liao, Yao Guan, Xuebo Yin, Chuanwei Zhu, Jin Liang, and Zhikui Guo

Cite This: *Environ. Sci. Technol.* 2023, 57, 21438−21447

Read Online

ACCESS | Metrics & More | Article Recommendations | Supporting Information

ABSTRACT: Deep-sea mining magnifies the release of heavy metals into seawater through oxidative dissolution of seafloor massive sulfide (SMS). At present, there is little information about how the metals released into seawater might be affected by the mineral assemblages, seawater conditions, and solid percentages. Here, leaching experiments were carried out to examine the behavior of three sulfides from the Southwest Indian Ridge, under conditions that replicated deep and shallow seawater environments at three solid−liquid ratios. The results demonstrated that sphalerite dissolved rapidly, and the metals released in both experimental conditions were comparable, potentially reflecting galvanic interactions between the sulfide minerals. Large quantities of the released metals were removed from the solutions when hydrous ferric oxides formed, especially for shallow seawater conditions. A comparison of metal concentrations in the leachates with the baseline metal concentrations in natural seawater indicated that most of the released metals, when diluted with seawater, would not have widespread impacts on ecosystems. Based on the obtained unique oxidative dissolution properties of each SMS at variable solid−liquid ratios, targeted wastewater discharge treatments are proposed to minimize impacts from the dissolved metals. This study will support the development of robust guidelines for deep-sea mining activities.

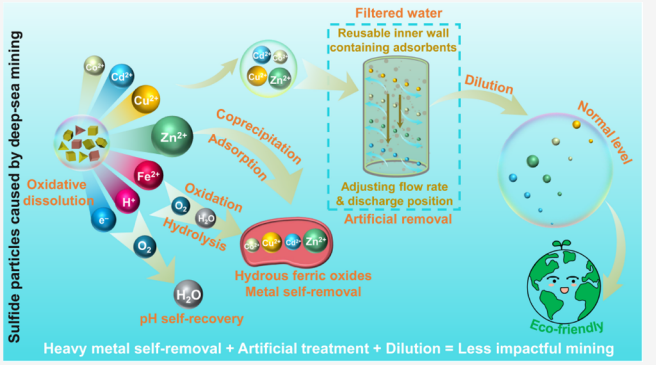

KEYWORDS: *seafloor massive sulfide, oxidative dissolution, heavy metals, leaching experiment, deep-sea mining, galvanic interaction*

INTRODUCTION

The global mining industry has expressed widespread interest in seafloor massive sulfide (SMS) deposits because of their potential as available metal resources.[1−4] However, the information available about the procedures proposed by the industry to mine SMS deposits suggests that there is potential to introduce large quantities of fresh sulfide particles into deep seawater during cutting and dewatering and into surface seawater because of accidental leakages (Figure S1).[5,6] These sulfide particles, once released, may undergo oxidative dissolution, thereby releasing heavy metals, and generating heavy metal-contaminated seawater around mining sites, with negative impacts on surrounding marine ecosystems.[7−12] Therefore, before large-scale mining activities are launched, the leachability of heavy metals from sulfide particles into seawater during the mining processes should be fully understood.

To date, numerous researchers have investigated the risk of metals leaching from sulfides into seawater.[12−17] However, the observations from most of these studies were derived from leaching experiments at a single solid−liquid ratio and at normal atmospheric temperatures and oxygen concentrations, with reaction times from several minutes to several hours. It has been suggested that sulfide dissolution rates are higher in surface seawater than in deep seawater because of the higher temperatures and oxygen concentrations.[12] The amount of sulfide particles in mining wastewater depends on shipboard mining operations, and the wastewater is diluted once discharged into seawater. Despite the research efforts to date, there is little information about how dissolved heavy metals might accumulate in the water column over time with variable percentages of solids. In addition, previous studies have mainly focused on SMS samples collected from hydrothermal fields on back-arc basins[12−15] and slow-spreading ridges.[16] The mineral assemblages, chemical compositions, and potential toxicity of SMS deposits from different tectonic settings are quite

Received: September 12, 2023
Revised: November 16, 2023
Accepted: November 16, 2023
Published: December 5, 2023

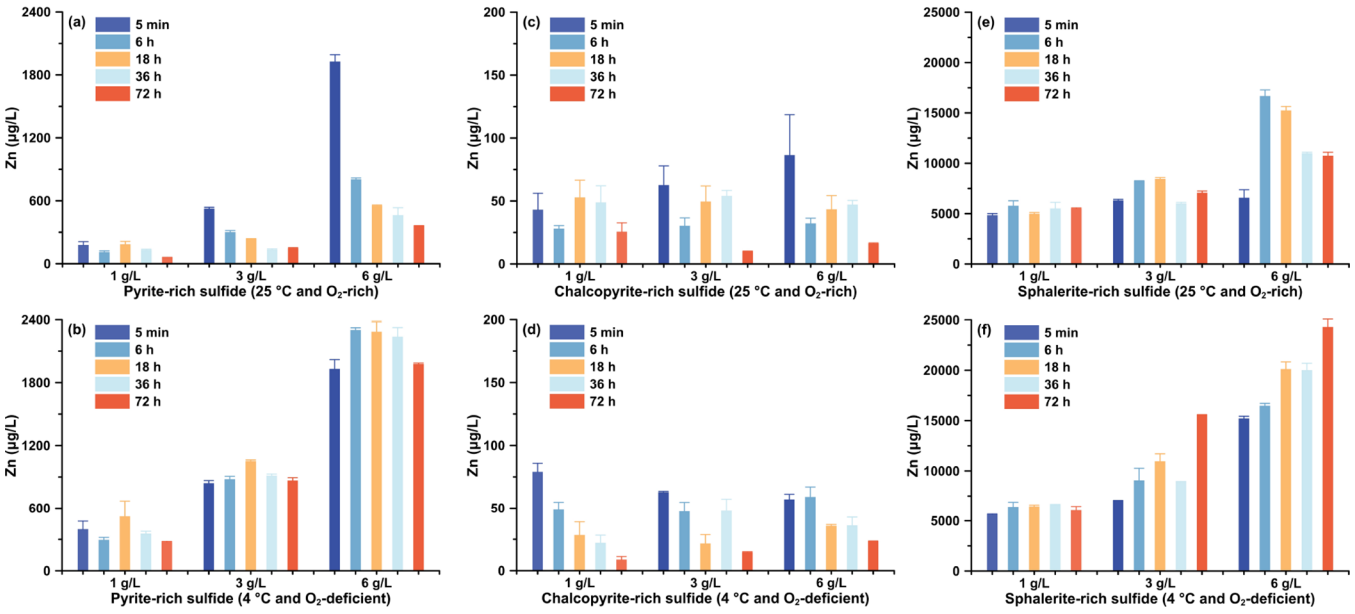

Figure 1. Temporal changes in the net accumulation of dissolved Zn concentrations in the leachates of the studied sulfides under different experimental conditions. The plots show the average values of duplicates, and error bars represent the standard deviation.

different.[18] For example, the abundant sulfosalts (e.g., orpiment), galena, and Fe-rich sphalerite that form from arc-related SMS deposits present high risks of As, Sb, Pb, and Hg toxicity.[18] Superlarge SMS deposits potentially form at ultraslow-spreading ridges.[4] Currently, the potential for heavy metal leaching from sulfides that form in such settings remains poorly understood.

The Southwest Indian Ridge (SWIR) is an ultraslow-spreading ridge.[19,20] Mineral resource assessments showed that the hydrothermal fields in the SWIR have great potential as a source of metals. For example, the SMS reserves in the Yuhuang hydrothermal field were estimated at $\sim 10.6 \times 10^6$ tonnes.[4] In this study, leaching experiments were carried out using pyrite-rich, chalcopyrite-rich, and sphalerite-rich sulfides collected from the SWIR to determine how heavy metals would release from fine sulfide particles suspended in seawater under different solid−liquid ratios, temperatures, and redox conditions, with the aim of clarifying how heavy metals would accumulate in different seawater environments during oxidative dissolution of sulfide minerals. The results from this study will provide a basis for optimizing the deep-sea mining processes and will contribute to achieving less impactful deep-sea mining.

MATERIALS AND METHODS

Sample Preparation. Three sulfide samples (T23, T5, and T3) were collected from the SWIR (Figure S2) using a Television-grab. These samples were stored at −18 °C during and after transportation to the laboratory until the leaching experiments were carried out. The altered or oxidized surface layers of each sample were cut and polished (Figure S3), and fresh portions were freeze-dried under vacuum conditions. The ore samples were ground to powder in a sealed tank using an agate ball-milling machine and then were immediately vacuum packed and stored at −18 °C to avoid oxidation. Sections of each sulfide were also prepared for mineralogical and geochemical analyses.

Mineralogical and Geochemical analyses. The mineralogy of the samples was identified by using a light microscope and X-ray diffraction (XRD). The chemical compositions of the samples were analyzed using inductively coupled plasma optical emission spectrometry (ICP-OES) and ICP-mass spectrometry (ICP-MS), and the chemical compositions of the pyrite, chalcopyrite, and sphalerite were determined using an electron probe microanalyzer and a laser ablation-ICP-MS. Details for these analyses are given in Texts S1−S4.

Leaching Experiments. The powdered samples were sieved to 2.5−45 μm to reflect the grain size of sulfide particles that would be found suspended in seawater after deep-sea mining[16] and then were tested for their freshness (Text S5 and Figures S4−S6). The leaching experiments were carried out under two conditions, namely, oxygen-rich at 25 °C to represent oxidation dissolution in shallow seawater (fast oxygen supply and high temperature) and oxygen-deficient at 4 °C to represent oxidation dissolution in deep seawater (slow oxygen supply and low temperature). Details for setting the experimental conditions are given in Text S6.

The leaching experiments were carried out at three solid−liquid ratios (1, 3, and 6 g/L), prepared by mixing 20, 60, and 120 mg of the powdered sulfide particles with 20 mL of natural Indian Ocean (IO) seawater in 50 mL acid-cleaned polypropylene centrifuge tubes. The tubes containing the reaction mixtures were shaken gently under each condition for 5 min and 6, 18, 36, and 72 h. All of the leaching experiments were carried out in duplicate. Once the reaction time was reached, the reacted seawater-mineral particle suspensions were filtered through 0.22-μm PTFE membrane filters. The resulting 180 seawater leachates and blank IO seawater were analyzed for dissolved metals and S using ICP-OES and ICP-MS. The detailed pretreatment and analysis processes are described in Text S7.

The pH values of the leachates were measured by using a pH meter (INESA, PHSJ-3F). Scanning electron microscopy (SEM) with energy-dispersive X-ray spectroscopy (EDS), X-ray photoelectron spectroscopy (XPS), and Mössbauer spectroscopy were employed to characterize the evolution of minerals in the separated solid residues at the end of the reaction (Texts S8−S10).

https://doi.org/10.1021/acs.est.3c07507
Environ. Sci. Technol. 2023, 57, 21438−21447

RESULTS AND DISCUSSION

Mineral Phases and Compositions of the Studied Sulfides. The mineral assemblages of the samples are shown in Figures S6 and S7 and Table S1. The sulfide minerals in T23 are dominated by pyrite (20%−30%) with minor sphalerite (~5%). T5 is a high-grade Cu ore, mainly consisting of chalcopyrite (>95%) with tiny amounts of sphalerite. The major sulfide minerals in T3 are sphalerite (60%−65%) and small amounts of pyrite (10%−15%). To reflect the dominant sulfide minerals, T23, T5, and T3 were defined as pyrite-rich, chalcopyrite-rich, and sphalerite-rich sulfides, respectively. The chemical compositions of the samples are shown in Tables S2. They contained various economically interesting metals at different contents, such as Cu (150 μg/g to 37.3 wt %) and Zn (654 μg/g to 46.8 wt %), and were also enriched with other metal(loid)s, such as V, Mn, Co, Ni, As, Mo, Cd, and Pb.

Leachability of Heavy Metals from Hydrothermal Sulfides. The net metal concentrations that accumulated in the solutions (i.e., the gross metal concentration minus the background value of the IO seawater) during the reactions under different experimental conditions are shown in Table S3. The Zn concentrations in the leachates of the three sulfides under all the experimental conditions increased sharply within the first 5 min (Figure 1), with the net accumulation of Zn reaching 83.8 ± 18.2% (n = 18) of the peak concentrations. The Zn concentrations in the seawater under oxygen-deficient conditions at 4 °C after 5 min were 1.44 ± 0.55 times (n = 9) higher than those in oxygen-rich conditions at 25 °C. Sphalerite, found in the three sulfides, is the main carrier of Zn (Table S4). The results indicate that oxidative dissolution of sphalerite in seawater occurred rapidly, and the amounts of Zn released during the leaching experiments under both seawater conditions were comparable.

The rapid dissolution of sphalerite in the initial oxidation stages may have been attributable to galvanic interactions.[21−23] A galvanic cell forms when two different sulfide minerals come into contact in the presence of an electrolyte (e.g., seawater). The mineral with lower rest potential acts as the anode and is rapidly dissolved, and the mineral with higher rest potential acts as the cathode and is galvanically protected (Figure S8).[21−23] Pyrite, chalcopyrite, and sphalerite were the major sulfide minerals in this study. Their rest potentials in solutions follow the order pyrite > chalcopyrite > sphalerite, regardless of the pH conditions (Figure S8).[24,25] Previous studies have confirmed that sphalerite dissolution and Zn release significantly increased in the presence of pyrite.[23,26] The Cu concentrations in the chalcopyrite-rich sulfide leachates were extremely low after 5 min (Figure S9), which likely suggests that chalcopyrite was galvanically protected. The Mössbauer spectroscopy results, especially for sphalerite-rich sulfide, showed that after reaction with seawater, the percentage of sphalerite clearly decreased relative to pyrite (Figure S10 and Table S5), likely indicating that pyrite was galvanically protected even after 72 h. Therefore, the galvanic effects triggered by pyrite−sphalerite or chalcopyrite−sphalerite coupling should have caused the preferential oxidation of sphalerite in the initial oxidation stages.

The net accumulation of Zn peaked in most of the reacted solutions between 5 min and 18 h and then gradually decreased (Figure 1). The decreases were particularly obvious in the experiments under oxygen-rich conditions at 25 °C and the Zn concentrations in the leachates from pyrite-rich, chalcopyrite-rich, and sphalerite-rich sulfides after 72 h were 26.4 ± 5.7%, 27.7 ± 14.7%, and 81.3 ± 12.8% of their corresponding peak concentrations. These results indicate that Zn was somehow separated from the solution at a removal rate that was higher than the release rate.

The sulfide samples had very high Fe contents (10.9−30.5 wt %), and the main carriers of Fe were pyrite (45.7 ± 1.5 wt %; n = 35), sphalerite (11.8 ± 2.9 wt %; n = 20), and chalcopyrite (30.8 ± 0.3 wt %; n = 10) (Table S4). Large amounts of Fe would have been released during oxidative dissolution of sulfide minerals (e.g., the galvanic dissolution of Fe-rich sphalerite; eq 1).[25]

$$Zn_aFe_{(1-a)}S \rightarrow Zn_a^{2+} + Fe_{(1-a)}^{2+} + S^0 + 2e^- \quad (1)$$

However, by the end of the experiments, the Fe had almost disappeared from most of the reacted solutions (<10 μg/L) (Figure S11). The almost-complete absence of Fe from the solutions suggests that, as reported elsewhere, the Fe(II) released was first oxidized into Fe(III), which has a low solubility in seawater, and then was hydrolyzed and precipitated as the hydrous ferric oxides (HFOs) that were thermodynamically suitable for the conditions.[12,16,27] SEM-EDS results of the solid residues showed that many insoluble compounds, mainly composed of Fe, O, Si, and S (Figure S12), were present, which suggests that HFOs likely formed, and the enrichment of Si may reflect the fact that HFOs usually combine with dissolved silica to enhance their stability in natural waters.[28,29] Compared with fresh sulfide samples, the XPS Fe $2p$ peaks of the solid residues exhibited a significant enhancement in the region of 711−714 eV and a significant reduction in the region of 707−708 eV (Figure S13), indicating that the Fe released was transformed into HFOs.[30−33] The formation of HFOs has also been confirmed by the presence of one doublet with IS = 0.39 mm/s, QS = 0.86 mm/s in the fitting results for the Mössbauer spectrum of the leached pyrite-rich sulfide (Figure S10 and Table S5).[34,35]

HFOs have high surface area and specific affinity for heavy metal adsorption or coprecipitation and so can regulate the concentrations of dissolved metals in aqueous systems.[36−38] Other researchers have reported that metals were adsorbed rapidly by HFOs.[39] Thus, Zn was mainly removed through adsorption or sequestration by HFOs, which is also reinforced by the finding that many compounds (~1 μm) comprising Zn, Fe, O, Si, and S were detected during SEM-EDS analysis (Figure S14). To better understand this process, Figure S15 summarizes the oxidative dissolution of sulfide minerals and the subsequent metal release and removal using Fe-rich sphalerite as an example. Consistent with this finding, researchers elsewhere reported that the natural oxides derived from SMS oxidation were significantly enriched with Zn (1.17 ± 0.34 wt %) and Si (11.09 ± 8.03 wt %).[40]

The Mössbauer parameters of the leached sphalerite-rich sulfides indicate that more sphalerite was dissolved in oxygen-rich conditions at 25 °C than that in oxygen-deficient conditions at 4 °C (Table S5). The leachates from the oxygen-rich conditions at 25 °C contained less dissolved Zn than the leachates from the oxygen-deficient conditions at 4 °C, especially for the pyrite-rich and sphalerite-rich sulfides (Figure 1). This was perhaps triggered by the more rapid supply of dissolved oxygen to form more HFOs (Figure S13), as other studies have reported Zn adsorption increased sharply as the formation of HFOs increased in aerated conditions.[41,42]

https://doi.org/10.1021/acs.est.3c07507
Environ. Sci. Technol. 2023, 57, 21438−21447

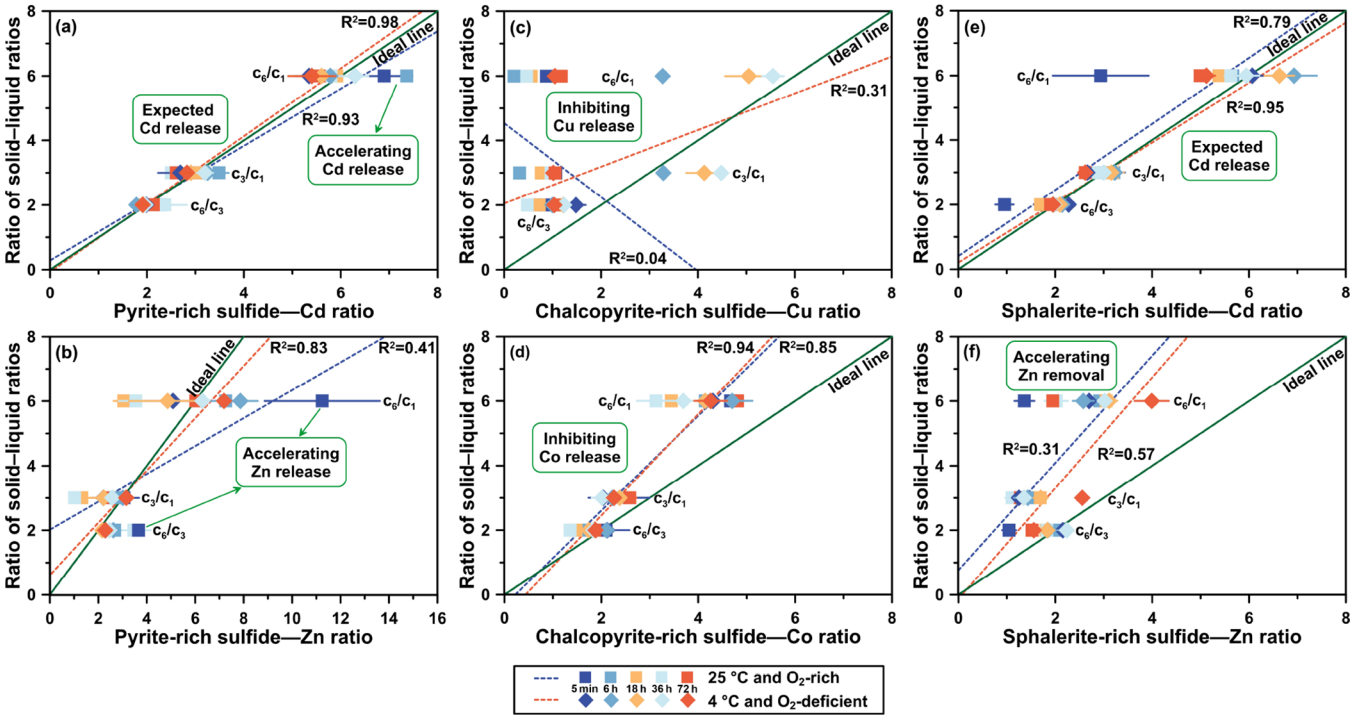

Figure 2. Correlations between the experimental solid−liquid ratio (SLR) and the net accumulation of dissolved heavy metals (after deducting the concentrations of natural seawater) in the leachates. C_aM/C_bM represents the ratio of metal M in the leachates under an experimental SLR for a g/L and b g/L. The plots show the average values of the duplicates, and error bars represent the standard deviation. The Cu concentrations in the chalcopyrite-rich sulfide leachates from the oxygen-deficient conditions at 4 °C after 5 min were extremely low (0.25 μg/L), so the related data points were deleted to improve the graphical effects.

The Cu, Cd, and Co concentrations in the leachates from all of the experimental conditions gradually increased over time (Figures S9, S16, and S17). This indicates that the metal fixation rate was less than or equal to the release rate, and does not mean that there was no removal of these metals. There are various reasons why the removal of these metals over time were less than that of Zn. The adsorption efficiency of Cd by HFOs is lower than that of Zn in the seawater conditions (pH = ∼8) and would have been higher in more alkaline conditions.[43] The pH values of the reacted solutions gradually increased over time (Figure S18); note that the affinity of Cu for HFOs in alkaline conditions may decrease as the pH increases.[43] In addition, previous aeration experiments suggested that the dissolved Zn was more easily removed than Co, with Zn and Co removal percentages of >60% and <20%, respectively.[41,42]

The Cu release was the highest from the chalcopyrite-rich sulfide, but the Cu concentrations did not increase significantly until after 18 h (Figure S9c,d). Chalcopyrite is the main carrier of Co for T5 (Table S4), and the Co content in T5 was ∼80 times higher than that in T23 (Table S2). However, the Co concentrations in the chalcopyrite-rich sulfide leachates were lower than those in the pyrite-rich sulfide leachates under a given experimental condition (Figure S17). These results suggest that the chalcopyrite had a relatively slow oxidation rate, mainly because T5 did not contain minerals with high rest potentials (e.g., pyrite) that could form galvanic cells to facilitate anodic dissolution of chalcopyrite.[23]

In general, chalcopyrite leached slowly at low temperatures and oxygen concentrations.[44] Interestingly, the Cu concentrations in the chalcopyrite-rich sulfide leachates from the oxygen-deficient conditions at 4 °C after 72 h were 1.29 ± 0.06 (n = 3) times greater than those from the oxygen-rich conditions at 25 °C. In addition, Mössbauer parameters demonstrate that more chalcopyrite remained in the leached chalcopyrite-rich sulfide from oxygen-rich conditions at 25 °C than that from oxygen-deficient conditions at 4 °C (Table S5). This might be associated with that the hydrogen ions generated from the galvanic dissolution of sphalerite (eq 2) that coupled with chalcopyrite in the oxygen-deficient conditions at 4 °C were consumed slowly (eqs 3 and 4).[24,25,44] The leaching of chalcopyrite increased in the presence of more hydrogen ions.[44]

$$S^0 + \frac{3}{2}O_2 + H_2O \rightarrow 2H^+ + SO_4^{2-} \quad (2)$$

$$O_2 + 4H^+ + 4e^- \rightarrow 2H_2O \quad (3)$$

$$2Fe^{2+} + 2H^+ + \frac{1}{2}O_2 \rightarrow 2Fe^{3+} + H_2O \quad (4)$$

The Pb, V, Mo, and Ni concentrations in the leachates remained very low throughout, and there were clear contrasts in the metal concentrations between the leachates and IO seawater (Figures S19−S22). Unlike arc-related sulfides significantly enriched with Pb,[12,15] the Pb contents of the SWIR samples were low (6.4−43.5 μg/g), mainly because the lack of Pb-bearing minerals, especially galena.[45] The net accumulations of Pb in the leachates were almost all negative (−0.24 ± 0.27 μg/L) (Figure S19). It was suggested that almost all the Pb(II) was adsorbed onto HFOs when the pH > 6 at 25 °C.[43] Therefore, almost all of the released Pb was removed by HFOs. Note that the net accumulations of V in the leachates were consistently negative (−2.16 ± 1.13 μg/L) (Figure S20), which suggests that oxidation products have the

https://doi.org/10.1021/acs.est.3c07507
Environ. Sci. Technol. 2023, 57, 21438−21447

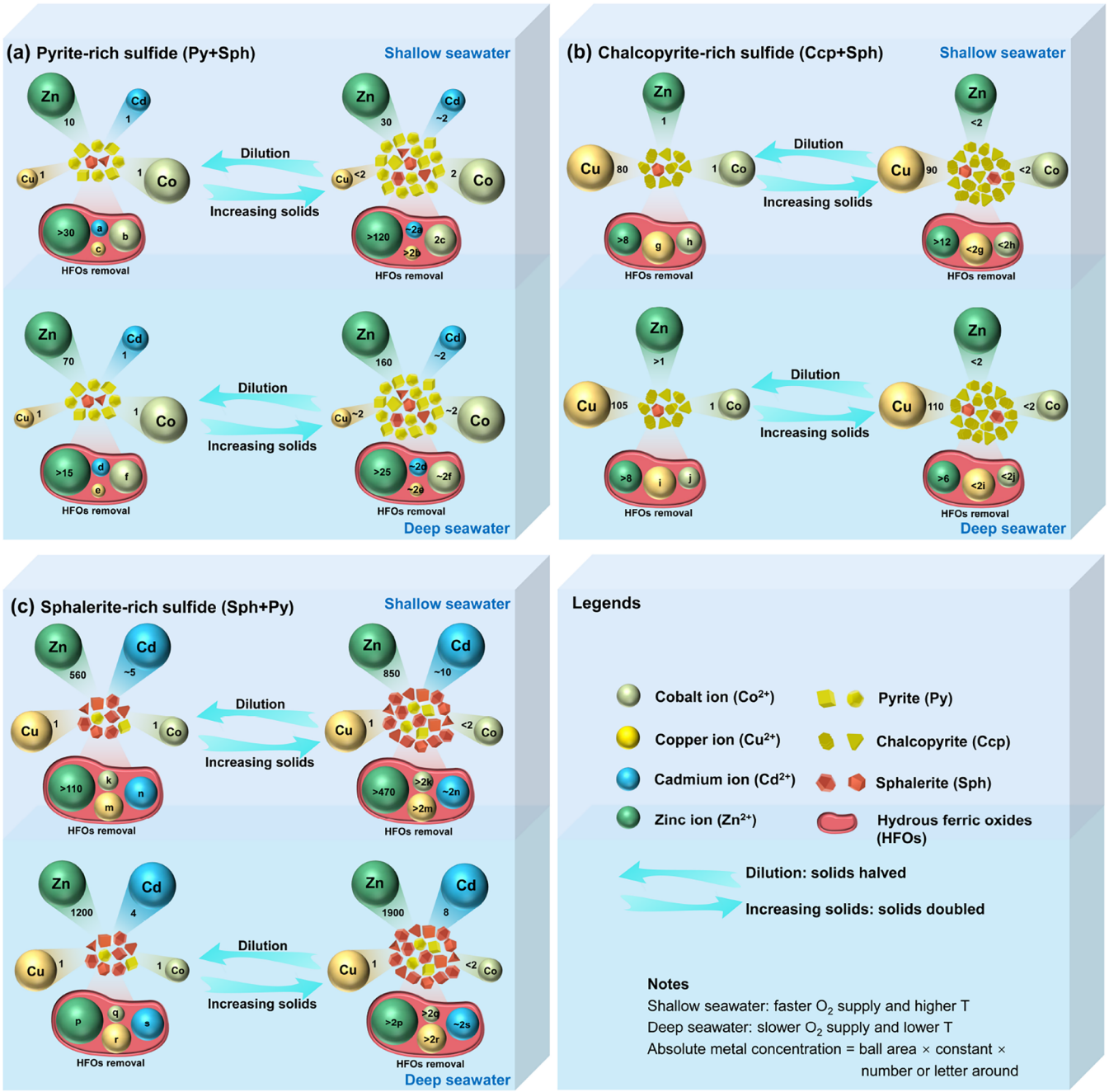

Figure 3. Generic models for the net accumulation of dissolved heavy metals in the water column during oxidative dissolution of sulfide particles similar to those examined in this study after deep-sea mining. The absolute concentration of a given metal is the product of the ball area, the coefficient near the ball, and a constant, and all the coefficients were based on data of dissolved metal concentrations obtained in experiments with solid−liquid ratios of 3 and 6 g/L. For metals that reached their peak concentrations within 72 h, the minimum concentrations of the released metals that were removed by HFOs were calculated. For metals that did not reach their peak concentrations within 72 h, lowercase letters were used to represent the concentrations at which they were removed. The differences in concentrations of the metals released from the three sulfides under different seawater conditions when either dilution occurs or the solid−liquid ratio increases can be seen by comparing the coefficients.

potential to scavenge V that is either released from sulfide or is already in seawater. There was a net accumulation of Mo (0.08 to 5.93 μg/g) and Ni (0.26 to 4.96 μg/g) in the reacted solutions, but their concentrations all decreased and were approaching 0 μg/L after 72 h (Figures S21 and S22), indicating a net removal of these metals by HFOs. Elsewhere, it has been reported that secondary oxides became enriched with Pb, V, Mo, and Ni during the submarine oxidative weathering of SMSs,[40] which reinforces the above findings.

Changes in the Dissolved Metal Concentrations at Variable Solid−Liquid Ratios. The leaching experiments were carried out at three solid−liquid ratios, providing an opportunity to compare the variations in the accumulation of metals in seawater when discharged sulfide particles increase in concentration or are diluted by seawater. For example, whether the net accumulation of each metal in seawater was six times higher for a solid−liquid ratio of 6 g/L than at 1 g/L, and vice versa.

https://doi.org/10.1021/acs.est.3c07507
Environ. Sci. Technol. 2023, 57, 21438−21447

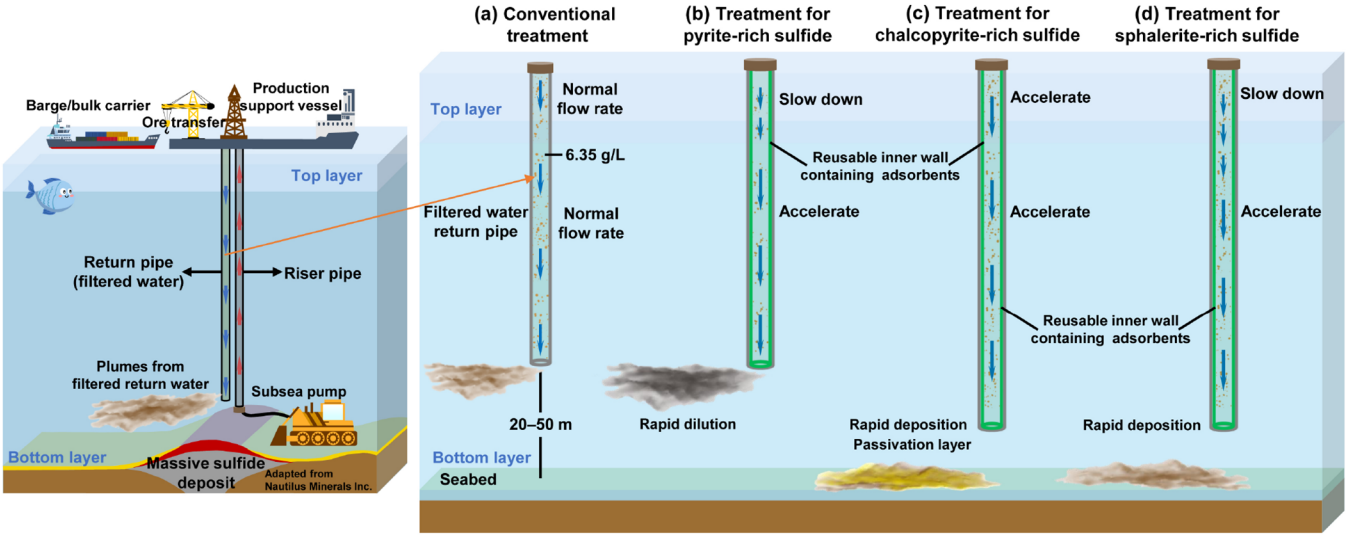

Figure 4. Targeted treatments to mitigate the adverse effects from mining wastewater that account for the dissolution behavior of the sulfides examined in this study.

The increases in the Zn, Cd, and Co concentrations in the pyrite-rich sulfide leachates under oxygen-rich conditions at 25 °C were greater than the increases in the solid−liquid ratio in the first 5 min or 6 h (Figure 2a,b and Figure S23a). This suggests that the release rates of Zn, Cd, and Co increased in the early stage when more pyrite-rich sulfide was added to seawater. Further, the Zn concentrations increased more rapidly than the Cd and Co concentrations (Figure 2a,b and Figure S23a). The changes in the Cd and Co concentrations in the pyrite-rich sulfide leachates under oxygen-deficient conditions at 4 °C were consistent with the changes in the solid−liquid ratio, but the Zn concentration in the reacted seawater after 72 h was higher than expected (Figure 2a,b and Figure S23a). Here, the pyrite-rich sulfide was mainly composed of pyrite with minor sphalerite (Figure S7a), and sphalerite is the main source of Cd.[46,47] The pyrite from the study area has a relatively high Zn content (~400 μg/g, n = 35; Table S4). Therefore, Zn in the solutions may come from sphalerite and another source (i.e., pyrite). Mössbauer parameters showed that the leached pyrite-rich sulfide had a lower proportion of Fe from pyrite than the pristine sample (Table S5). These results suggest that as the solid−liquid ratio increased, the dissolution rate of sphalerite in seawater under oxygen-rich conditions at 25 °C increased, and more pyrite-derived Zn was released in both seawater conditions. However, more Zn remained in the deep seawater solutions than in the shallow seawater solutions because of the low oxygen supply and low removal efficiency (Figure 2b).[41]

The ratios of the Cu, Co, and Zn concentrations in the chalcopyrite-rich sulfide leachates under variable solid percentages are plotted to the left of the expected lines (Figure 2c,d and Figure S23b). As the solid−liquid ratio increased from 1 to 6 g/L, the final net accumulated Cu concentrations increased from 957 to 1129 μg/L in the shallow seawater conditions and from 1295 to 1358 μg/L in the deep seawater conditions (Figure S9c,d). These results indicate that the oxidation of the chalcopyrite-rich sulfide may have been inhibited as the solid−liquid ratio increased. This may have been caused by chalcopyrite passivation, where intermediates (i.e., low-solubility Cu polysulfide and or elemental sulfur) that form during chalcopyrite oxidation may serve as an insulating film and may limit the overall chalcopyrite dissolution reactions.[48,49] The presence of components with Cu and Fe concentrations significantly higher than and lower than those of the chalcopyrite on the surface of the oxidation residues likely indicated the formation of such compounds (Figure S24). Similarly, the results from a previous study showed that chalcopyrite dissolution was inhibited as the pulp density increased from 0.5% to 5%.[50]

The increases in the Zn and Co concentrations in the sphalerite-rich sulfide leachates were less than the increases in the solid−liquid ratios (Figure 2f and Figure S23c), and the changes in the Cd concentrations were consistent with the changes in the solid−liquid ratios (Figure 2e). Cd was mainly present as an isomorphous impurity in sphalerite,[46,47] while Zn was also present in other minerals (e.g., pyrite), so the increases in the Zn concentrations should be similar to, or greater than, the increases in the Cd concentrations that corresponded with the increases in the solid−liquid ratios. The amounts of sphalerite dissolution and HFO precipitation increased when the solid−liquid ratio of the leaching experiments increased. Cd removal by HFOs is optimal at a higher pH than Zn and Co removal.[42,43] Therefore, the lower-than-expected Zn and Co concentrations in the reacted solutions more likely reflect an increase in the adsorption efficiency by HFOs. The metal concentration ratios in leachates from oxygen-rich conditions at 25 °C were low, suggesting that more Zn and Co were removed under the shallow seawater conditions. The generic models for the net accumulation of heavy metals in the water column during oxidative dissolution of different sulfide particles at variable solid−liquid ratios are summarized in Figure 3.

Acid Generation and Sulfur Release. Hydrogen ions are generally released into the surrounding aquatic environment during oxidative dissolution of sulfide minerals (Table S6).[51,52] However, other chemical reactions may also help to regulate acid levels in solutions (eqs 3 and 4).[44]

The pH values in the leachates of the pyrite-rich and sphalerite-rich sulfides decreased rapidly in the first 5 min and then increased gradually in both seawater conditions (Figure S18a,c). This suggests that acid is rapidly generated once pyrite-rich and sphalerite-rich sulfides come into contact with

https://doi.org/10.1021/acs.est.3c07507
Environ. Sci. Technol. 2023, 57, 21438−21447

seawater, but with the occurrence of chemical reactions that consume acid (eqs 3 and 4), the seawater pH will revert toward normal levels over time. The pH values of the chalcopyrite-rich sulfide leachates were close to or higher than the pH of the initial seawater (7.77 ± 0.01) for all the conditions (Figure S18b), which suggests that the oxidative dissolution of chalcopyrite-rich sulfide caused very little accumulation of acid in seawater. More details about the acid accumulation in the chalcopyrite-rich sulfide leachates over time are provided in Text S11.

As sulfide minerals oxidize, dissolved S can be released into seawater (Table S6). Dissolved S accumulated in all leachates, with higher concentrations of dissolved S in the oxygen-rich conditions at 25 °C than in the oxygen-deficient conditions at 4 °C (Figure S25). This is mainly because elemental S released by galvanic oxidation was more easily to be oxidized to SO_4^{2-} in the oxygen-rich conditions than in the low-oxygen conditions (eq 2).[44]

Risk Assessment and Mitigation Measures for Mining Similar SMS Deposits. Human activities (e.g., mining and smelting) have released large amounts of heavy metals into surrounding air, soil, and water, causing increasingly severe heavy metal pollution. These heavy metals can reach the oceans through rivers, runoff, and atmospheric deposition, ultimately resulting in marine heavy metal pollution.[53−55] SMS deposits are likely to be mined commercially in the future[3,56] and may also generate heavy metal-contaminated seawater. To reduce the adverse effects on marine ecosystems caused by the discharge of wastewater at the sea surface, such as turbidity clouds and algal blooms, it was suggested that substantial quantities of filtered water containing suspended particles with a solid−liquid ratio of 6.35 g/L could be discharged into deep seawater at 25−50 m above the seabed (Figure 4a).[56,57]

Through statistical analysis, based on a solid−liquid ratio of 6 g/L in the filtered water and the environmental baseline metal and S concentrations in natural IO seawater, the results showed that the dissolved Fe, Pb, V, Mo, Ni, and S needed to be diluted no more than several times to reach their normal concentrations in natural seawater. The environmental damage from these elements is likely to be minimal because seawater has huge dilution and buffering capabilities.[58−60] Zn, Cd, and Co from pyrite-rich and sphalerite-rich sulfides and Cu and Co from chalcopyrite-rich sulfide under both seawater conditions have higher dilution requirements, ranging from dozens to thousands of times. Zn, Cd, Co, and Cu are essential micronutrients for marine phytoplankton.[61,62] At appropriate concentrations, they can promote the growth of phytoplankton and improve marine primary productivity, but can cause toxicity to phytoplankton and inhibit their growth at excessive concentrations.[61,62] Therefore, to reduce the accumulation of these metals in the water column over wide areas during deep-sea mining, unnecessary leakages should be avoided, and the recovery rates should be improved.

Different types of sulfides exhibit unique patterns of oxidative dissolution and release heavy metals differently under different solid−liquid ratios because of variations in the mineral assemblages. In addition, dissolved metals are released rapidly (Figure S26), but their concentrations will be regulated by the formation of HFOs and will generally be removed more efficiently in shallow seawater than in deep seawater. These findings can be used to optimize the currently proposed mining model, especially in refining wastewater treatment processes. The risk of pollution from Zn, Cd, Co, and Cu can be further mitigated.

For pyrite-rich sulfide, the pyrite oxidation increased as the solid−liquid ratio increased, thereby increasing the release of pyrite-derived Zn. This will lead to the removal of more heavy metals from the shallow seawater; more Zn will remain in the deep seawater (Figure 3a). To reduce the risks of heavy metal pollution when mining this type of sulfide (i.e., T23), the flow rate of filtered water can be controlled to prolong the residence time of solids in the shallow seawater. The flow rate of filtered water can be accelerated in deep seawater, so that sulfide particles are quickly diluted by seawater after being discharged from the return pipe (Figure 4b).

The total oxidation rate of chalcopyrite-rich sulfide decreased sharply as the percentage of solids increased (Figure 3b). The risk of pollution from heavy metals (e.g., Cu and Co) when mining SMS similar to T5 can be mitigated by allowing more chalcopyrite-rich sulfide particles to gather together. This can be achieved by appropriately accelerating the flow rate of filtered water and positioning the discharge outlet close to the seabed so that the chalcopyrite-rich sulfide particles will be deposited rapidly and a chalcopyrite passivation layer will be formed to avoid extensive oxidation (Figure 4c).

The net accumulated Cd concentrations suggest that the oxidation rate of sphalerite-rich sulfide did not change much as the solid−liquid ratios changed. However, the amounts of Zn and Co attenuated from seawater are likely to increase as the solid−liquid ratio increases (Figure 3c). The flow rate of the return water can be controlled to extend the residence time of solids in shallow seawater, and the discharge outlet should be deep to facilitate rapid deposition of the solids on the seabed (Figure 4d). This would help to reduce the overall accumulation of heavy metals in seawater when mining SMS similar to T3.

Even slight acidification of the ocean environment has a detrimental impact on marine organisms and ecosystems.[63] Consistent with the findings of another study,[59] this study suggests that the oxidative dissolution of chalcopyrite-rich sulfide is unlikely to cause acid contamination (Figure S18b). Oxidative dissolution of pyrite-rich and sphalerite-rich sulfides in seawater was a rapid acidogenic process in both seawater conditions, but the pH of seawater with a relatively low solid−liquid ratio reverted to normal levels over time (Figure S18a,c). Therefore, as long as the discharged wastewater is diluted, the acid produced is unlikely to be problematic.

Predicting Heavy Metal Release from Deep-Sea Mining at a Global Scale. This study demonstrates that oxidative dissolution of sphalerite, which has a relatively low rest potential, occurred rapidly in seawater because of galvanic interactions (Figure S26). Sphalerite, a very common mineral, seems to be present in almost all SMS deposits in the midocean ridges, volcanic arcs, and back-arc spreading centers.[12,18,45,64] Galvanic dissolution of sphalerite is therefore likely to occur in all oceans, and the observations in this study have implications for heavy metal release from global-scale deep-sea mining.

Cd is mainly present as an isomorphous impurity in sphalerite.[46,47] Dissolved Cd seems to be more difficult than other metals to remove by HFOs (Figure S16); thus, it is possible to conduct a global estimation of the Cd release. The estimated abundance of existing SMS deposits in global oceans is ∼6×10^8 tonnes.[2] Globally, the calculated average Cd content in SMSs is ∼196 μg/g (n = 803).[12,45,64] Based on

https://doi.org/10.1021/acs.est.3c07507
Environ. Sci. Technol. 2023, 57, 21438−21447

these data, a functional relationship was established among Cd release, the exploitation rate, and the recovery rate (Figure S27). Assuming that 50% of the existing SMS deposits are extracted with a recovery rate of 80%, the maximum Cd release is ~7.44×10^3 tonnes.

Cd displays a nutrient-type distribution in global oceans, with concentrations depleted in shallow seawater (1−2 pmol/kg) and enriched in deep seawater (~1.1 nmol/kg).[65] High concentrations of Cd may cause toxicity to phytoplankton and reduce their reproduction rates.[61,66] Cd released from sphalerite dissolution may not influence the average level of Cd in the global oceans after it is diluted by seawater (~1.3×10^{21} kg) but may temporarily affect the biogeochemical Cd budgets around mining areas. Note that on first contact with seawater, sphalerite is oxidized and releases Cd very rapidly, but the rates of oxidation and Cd release decrease significantly as time passes (Figures S26). In other words, most sphalerite particles may undergo galvanic dissolution in the return pipe and release a large amount of Cd. The inner wall of the return pipe could be redesigned to contain reusable heavy metal adsorbents so that any free heavy metals released during the wastewater delivery could be adsorbed by the inner wall of the pipe (Figure 4). For example, large quantities of Cd could be removed by adsorption to the inner wall of a return pipe that containing porous hydrogel adsorbents.[67]

Environmental Implications for Future Deep-Sea Mining. The laboratory results from this study suggest that because of the potential impacts of galvanic interactions between the symbiotic sulfide minerals, fresh sulfide minerals with relatively low rest potentials will rapidly dissolve and release heavy metals, both in shallow and deep seawater environments during mining operations. The heavy metals that are released from sulfides or already in natural seawater may be adsorbed by the HFOs that form; this process is likely to be important for future deep-sea mining. This study also demonstrates that heavy metal removal by HFOs is higher in shallow seawater environments than in deep seawater environments, resulting in the accumulation of more dissolved heavy metals in deep seawater. Therefore, the previously proposed model that direct discharge of wastewater generated from mining SMS deposits into deep-sea environments may need to be optimized. Less impactful deep-sea mining is possible if individual measures are formulated for each SMS and adopted before or during mining activities. As reported elsewhere,[16] this study found that the risk assessments of a specific heavy metal should not be based on only the bulk geochemical composition of the SMS.

To gain additional insight into the fate of sulfide particles generated by deep-sea mining, it would be useful to consider the residence time of the suspended sulfide particles in seawater. Note that the leaching experiments were carried out under 1 atm of pressure (~0.1 MPa), but sulfide oxidation in actual deep-sea environments may be subjected to ~15 MPa (equivalent to a sampling location at approximately 1500 m deep). Pressure may also influence the speciation in seawater (e.g., hydrolysis and complexation) and the metal(loid) chemistry of the secondary precipitates (e.g., solubility, adsorption).[9,68] The possible variation suggests that it would be useful to investigate how pressure influences the chemical equilibrium of each heavy metal in deep-sea environments. Future studies could also explore the factors controlling the formation, stability, and adsorption capability of secondary HFOs, as well as the dietary exposure risk from metals retained in HFOs.[37,69−71] These additional studies contribute to improving the understanding of the risks of heavy metal pollution caused by deep-sea mining.

■ ASSOCIATED CONTENT

Supporting Information

The Supporting Information is available free of charge at https://pubs.acs.org/doi/10.1021/acs.est.3c07507.

Model for deep-sea mining; sampling locations; macrophotographs and XRD patterns of fresh sulfides; photomicrographs of sulfide minerals; pH values and dissolved metal and S concentrations of the leachates; SEM, XPS, and Mössbauer spectroscopy results; schematic diagrams for sulfide mineral dissolution; correlations between solid−liquid ratios and dissolved metal concentrations; models for Cd release; methods for mineralogical and geochemical analyses; details for setting experimental conditions, freshness checking of sulfide minerals, desalination processes for the leachates, and acid accumulation in the rich-chalcopyrite sulfide leachates; mineral assemblages of the samples; geochemical data for the sulfides, sulfide minerals, and the leachates; and chemical equations (PDF)

■ AUTHOR INFORMATION

Corresponding Author

Chunhui Tao − *Key Laboratory of Submarine Geosciences, Second Institute of Oceanography, Ministry of Natural Resources, Hangzhou 310012, China; School of Oceanography, Shanghai Jiaotong University, Shanghai 200030, China;* orcid.org/0000-0003-2173-6044; Phone: +86-571-88829003; Email: taochunhui@sio.org.cn

Authors

Siyi Hu − *Key Laboratory of Submarine Geosciences, Second Institute of Oceanography, Ministry of Natural Resources, Hangzhou 310012, China; Guangxi Key Laboratory of Beibu Gulf Marine Resources, Environment and Sustainable Development, Fourth Institute of Oceanography, Ministry of Natural Resources, Beihai 536000, China;* orcid.org/0000-0002-5945-8943

Shili Liao − *Key Laboratory of Submarine Geosciences, Second Institute of Oceanography, Ministry of Natural Resources, Hangzhou 310012, China*

Yao Guan − *Guangxi Key Laboratory of Beibu Gulf Marine Resources, Environment and Sustainable Development, Fourth Institute of Oceanography, Ministry of Natural Resources, Beihai 536000, China*

Xuebo Yin − *Key Laboratory of Marine Geology and Environment, Institute of Oceanology, Chinese Academy of Sciences, Qingdao 266071, China*

Chuanwei Zhu − *State Key Laboratory of Ore Deposit Geochemistry, Institute of Geochemistry, Chinese Academy of Sciences, Guiyang 550081, China*

Jin Liang − *Key Laboratory of Submarine Geosciences, Second Institute of Oceanography, Ministry of Natural Resources, Hangzhou 310012, China*

Zhikui Guo − *Key Laboratory of Submarine Geosciences, Second Institute of Oceanography, Ministry of Natural Resources, Hangzhou 310012, China*

Complete contact information is available at:

https://pubs.acs.org/10.1021/acs.est.3c07507

Notes

The authors declare no competing financial interest.

■ ACKNOWLEDGMENTS

The authors are grateful to the Associate Editor Dr. Jordi Dachs and the reviewers, for their valuable and constructive comments on the original manuscript, by which it was greatly improved. This work was supported by National Natural Science Foundation of China (Grant No. 42127807), Scientific Research Fund of the Second Institute of Oceanography, MNR (Grant Nos. JB2203, SZ2201), the China Postdoctoral Science Foundation (Grant No. 2021M693778).

■ REFERENCES

(1) Rona, P. A. Resources of the sea floor. *Science* **2003**, *299*, 673−674.
(2) Hannington, M.; Jamieson, J.; Monecke, T.; Petersen, S.; Beaulieu, S. The abundance of seafloor massive sulfide deposits. *Geology* **2011**, *39*, 1155−1158.
(3) Murton, B. J.; Lehrmann, B.; Dutrieux, A. M.; Martins, S.; de la Iglesia, A. G.; Stobbs, I. J.; Barriga, F. J. A. S.; Bialas, J.; Dannowski, A.; Vardy, M. E.; North, L. J.; Yeo, I. A. L. M.; Lusty, P. A. J.; Petersen, S. Geological fate of seafloor massive sulphides at the TAG hydrothermal field (Mid-Atlantic Ridge). *Ore Geol. Rev.* **2019**, *107*, 903−925.
(4) Yu, J.; Tao, C.; Liao, S.; Alveirinho Dias, Á.; Liang, J.; Yang, W.; Zhu, C. Resource estimation of the sulfide-rich deposits of the Yuhuang-1 hydrothermal field on the ultraslow-spreading Southwest Indian Ridge. *Ore Geol. Rev.* **2021**, *134*, No. 104169.
(5) Collins, P. C.; Croot, P.; Carlsson, J.; Colaço, A.; Grehan, A.; Hyeong, K.; Kennedy, R.; Mohn, C.; Smith, S.; Yamamoto, H.; Rowden, A. A primer for the Environmental Impact Assessment of mining at seafloor massive sulfide deposits. *Marine Policy* **2013**, *42*, 198−209.
(6) Narita, T.; Oshika, J.; Okamoto, N.; Toyohara, T.; Miwa, T. Summary of Environmental Impact Assessment for Mining Seafloor Massive Sulfides in Japan. *J. Shipping Ocean Eng.* **2015**, 103−114.
(7) Boschen, R. E.; Rowden, A. A.; Clark, M. R.; Gardner, J. P. A. Mining of deep-sea seafloor massive sulfides: A review of the deposits, their benthic communities, impacts from mining, regulatory frameworks and management strategies. *Ocean & Coastal Management* **2013**, *84*, 54−67.
(8) Boschen, R. E.; Rowden, A. A.; Clark, M. R.; Pallentin, A.; Gardner, J. P. A. Seafloor massive sulfide deposits support unique megafaunal assemblages: Implications for seabed mining and conservation. *Marine Environmental Research* **2016**, *115*, 78−88.
(9) Simpson, S. L.; Spadaro, D. A. Bioavailability and Chronic Toxicity of Metal Sulfide Minerals to Benthic Marine Invertebrates: Implications for Deep Sea Exploration, Mining and Tailings Disposal. *Environ. Sci. Technol.* **2016**, *50*, 4061−4070.
(10) Vare, L. L.; Baker, M. C.; Howe, J. A.; Levin, L. A.; Neira, C.; Ramirez-Llodra, E. Z.; Reichelt-Brushett, A.; Rowden, A. A.; Shimmield, T. M.; Simpson, S. L.; Soto, E. H. Scientific Considerations for the Assessment and Management of Mine Tailings Disposal in the Deep Sea. *Front. Mar. Sci.* **2018**, *5*, 17 DOI: 10.3389/fmars.2018.00017.
(11) Stauber, J. L.; Adams, M. S.; Batley, G. E.; Golding, L. A.; Hargreaves, I.; Peeters, L.; Reichelt-Brushett, A. J.; Simpson, S. L. A generic environmental risk assessment framework for deep-sea tailings placement. *Sci. Total Environ.* **2022**, *845*, No. 157311.
(12) Fuchida, S.; Ishibashi, J. i.; Shimada, K.; Nozaki, T.; Kumagai, H.; Kawachi, M.; Matsushita, Y.; Koshikawa, H. Onboard experiment investigating metal leaching of fresh hydrothermal sulfide cores into seawater. *Geochem. Trans.* **2018**, *19*, 1−15.
(13) Parry, D. L. *Solwara 1 Project Elutriate Report Phase 1 and 2*; Coffey Natural Systems Pty Ltd., 2008.
(14) Simpson, S.; Angel, B.; Hamilton, I.; Spadaro, D.; Binet, M. *Water and Sediment Characterisation and Toxicity Assessment for the Solwara 1 Project*; Environmental Impact Statement; Natural Minerals Inc., 2007.
(15) Fuchida, S.; Yokoyama, A.; Fukuchi, R.; Ishibashi, J.-i.; Kawagucci, S.; Kawachi, M.; Koshikawa, H. Leaching of metals and metalloids from hydrothermal ore particulates and their effects on marine phytoplankton. *ACS Omega* **2017**, *2*, 3175−3182.
(16) Fallon, E. K.; Niehorster, E.; Brooker, R. A.; Scott, T. B. Experimental leaching of massive sulphide from TAG active hydrothermal mound and implications for seafloor mining. *Mar. Pollut. Bull.* **2018**, *126*, 501−515.
(17) Knight, R. D.; Roberts, S.; Cooper, M. J. Investigating monomineralic and polymineralic reactions during the oxidation of sulphide minerals in seawater: Implications for mining seafloor massive sulphide deposits. *Appl. Geochem.* **2018**, *90*, 63−74.
(18) Fallon, E. K.; Frische, M.; Petersen, S.; Brooker, R. A.; Scott, T. B. Geological, Mineralogical and Textural Impacts on the Distribution of Environmentally Toxic Trace Elements in Seafloor Massive Sulfide Occurrences. *Minerals* **2019**, *9*, 162.
(19) Dick, H. J. B.; Lin, J.; Schouten, H. An ultraslow-spreading class of ocean ridge. *Nature* **2003**, *426*, 405−412.
(20) Tao, C.; Seyfried, W. E.; Lowell, R. P.; Liu, Y.; Liang, J.; Guo, Z.; Ding, K.; Zhang, H.; Liu, J.; Qiu, L.; Egorov, I.; Liao, S.; Zhao, M.; Zhou, J.; Deng, X.; Li, H.; Wang, H.; Cai, W.; Zhang, G.; Zhou, H.; Lin, J.; Li, W. Deep high-temperature hydrothermal circulation in a detachment faulting system on the ultra-slow spreading ridge. *Nat. Commun.* **2020**, *11*, 1300.
(21) Kwong, Y.; Swerhone, G. W.; Lawrence, J. R. Galvanic sulphide oxidation as a metal-leaching mechanism and its environmental implications. *Geochemistry Exploration Environment Analysis* **2003**, *3*, 337−343.
(22) Liu, Q.; Li, H.; Zhou, L. Galvanic interactions between metal sulfide minerals in a flowing system: Implications for mines environmental restoration. *Appl. Geochem.* **2008**, *23*, 2316−2323.
(23) Heidel, C.; Tichomirowa, M.; Junghans, M. Oxygen and sulfur isotope investigations of the oxidation of sulfide mixtures containing pyrite, galena, and sphalerite. *Chem. Geol.* **2013**, *342*, 29−43.
(24) Majima, H. How oxidation affects selective flotation of complex sulphide ores. *Can. Metall. Q.* **1969**, *8*, 269−273.
(25) Rao, S. R.; Finch, J. A. Galvanic Interaction Studies on Sulphide Minerals. *Can. Metall. Q.* **1988**, *27*, 253−259.
(26) Chopard, A.; Plante, B.; Benzaazoua, M.; Bouzahzah, H.; Marion, P. Geochemical investigation of the galvanic effects during oxidation of pyrite and base-metals sulfides. *Chemosphere* **2017**, *166*, 281−291.
(27) Liu, X.; Millero, F. J. The solubility of iron hydroxide in sodium chloride solutions. *Geochim. Cosmochim. Acta* **1999**, *63*, 3487−3497.
(28) Mayer, T. D.; Jarrell, W. M. Formation and stability of iron(II) oxidation products under natural concentrations of dissolved silica. *Water Res.* **1996**, *30*, 1208−1214.
(29) Wu, L.; Beard, B. L.; Roden, E. E.; Johnson, C. M. Stable Iron Isotope Fractionation Between Aqueous Fe(II) and Hydrous Ferric Oxide. *Environ. Sci. Technol.* **2011**, *45*, 1847−1852.
(30) Buckley, A. N.; Woods, R. An X-ray photoelectron spectroscopic Study of the oxidation of chalcopyrite. *Aust. J. Chem.* **1984**, *37*, 2403−2413.
(31) Smart, R. S. C. Surface layers in base metal sulphide flotation. *Miner. Eng.* **1991**, *4*, 891−909.
(32) Pratt, A. R.; Muir, I. J.; Nesbitt, H. W. X-ray photoelectron and Auger electron spectroscopic studies of pyrrhotite and mechanism of air oxidation. *Geochim. Cosmochim. Acta* **1994**, *58*, 827−841.
(33) Fairthorne, G.; Fornasiero, D.; Ralston, J. Effect of oxidation on the collectorless flotation of chalcopyrite. *Int. J. Miner. Process.* **1997**, *49*, 31−48.

(34) Oh, S. J.; Cook, D. C.; Townsend, H. E. Characterization of iron oxides commonly formed as corrosion products on steel. *Hyperfine Interact.* **1998**, *112*, 59−65.
(35) Murad, E.; Schwertmann, U. The Mössbauer spectrum of ferrihydrite and its relations to those of other iron oxides. *Am. Mineral.* **1980**, *65*, 1044−1049.
(36) Johnson, C. A. The regulation of trace element concentrations in river and estuarine waters contaminated with acid mine drainage: The adsorption of Cu and Zn on amorphous Fe oxyhydroxides. *Geochim.cosmochim.acta* **1986**, *50*, 2433−2438.
(37) Lu, X.; Wang, H. Microbial Oxidation of Sulfide Tailings and the Environmental Consequences. *Elements* **2012**, *8*, 119−124.
(38) Yan, X.; Zhu, M.; Li, W.; Peacock, C. L.; Ma, J.; Wen, H.; Liu, F.; Zhou, Z.; Zhu, C.; Yin, H. Cadmium Isotope Fractionation during Adsorption and Substitution with Iron (Oxyhydr)oxides. *Environ. Sci. Technol.* **2021**, *55*, 11601−11611.
(39) Balistrieri, L. S.; Murray, J. W. The adsorption of Cu, Pb, Zn, and Cd on goethite from major ion seawater. *Geochim. Cosmochim. Acta* **1982**, *46*, 1253−1265.
(40) Hu, S.; Tao, C.; Liao, S.; Zhu, C.; Qiu, Z. Transformation of minerals and mobility of heavy metals during oxidative weathering of seafloor massive sulfide and their environmental significance. *Sci. Total Environ.* **2022**, *819*, No. 153091.
(41) Cravotta, C. A. Passive aerobic treatment of net-alkaline, iron-laden drainage from a flooded underground anthracite mine, Pennsylvania, USA. *Mine Water Environ.* **2007**, *26*, 128−149.
(42) Burrows, J. E.; Cravotta, C. A.; Peters, S. C. Enhanced Al and Zn removal from coal-mine drainage during rapid oxidation and precipitation of Fe oxides at near-neutral pH. *Appl. Geochem.* **2017**, *78*, 194−210.
(43) Cravotta, C. A. Dissolved metals and associated constituents in abandoned coal-mine discharges, Pennsylvania, USA. Part 2: Geochemical controls on constituent concentrations. *Appl. Geochem.* **2008**, *23*, 203−226.
(44) Hackl, R.; Dreisinger, D.; Peters, E.; King, J. A. Passivation of chalcopyrite during oxidative leaching in sulfate media. *Hydrometallurgy* **1995**, *39*, 25−48.
(45) Liao, S.; Tao, C.; Li, H.; Barriga, F. J. A. S.; Liang, J.; Yang, W.; Yu, J.; Zhu, C. Bulk geochemistry, sulfur isotope characteristics of the Yuhuang-1 hydrothermal field on the ultraslow-spreading Southwest Indian Ridge. *Ore Geol. Rev.* **2018**, *96*, 13−27.
(46) Schwartz, M. O. Cadmium in Zinc Deposits: Economic Geology of a Polluting Element. *Int. Geol. Rev.* **2000**, *42*, 445−469.
(47) Zhu, C.; Wen, H.; Zhang, Y.; Yin, R.; Cloquet, C. Cd isotope fractionation during sulfide mineral weathering in the Fule Zn-Pb-Cd deposit, Yunnan Province, Southwest China. *Sci. Total Environ.* **2018**, *616*, 64−72.
(48) Munoz, P.; Miller, J.; Wadsworth, M. Reaction mechanism for the acid ferric sulfate leaching of chalcopyrite. *Metall. Trans. B* **1979**, *10*, 149−158.
(49) Córdoba, E. M.; Muñoz, J. A.; Blázquez, M. L.; González, F.; Ballester, A. Leaching of chalcopyrite with ferric ion. Part I: General aspects. *Hydrometallurgy* **2008**, *93*, 81−87.
(50) Córdoba, E. M.; Muñoz, J. A.; Blázquez, M. L.; González, F.; Ballester, A. Passivation of chalcopyrite during its chemical leaching with ferric ion at 68°C. *Miner. Eng.* **2009**, *22*, 229−235.
(51) Lee, J. S.; Chon, H. T. Hydrogeochemical characteristics of acid mine drainage in the vicinity of an abandoned mine, Daduk Creek, Korea. *J. Geochem. Explor.* **2006**, *88*, 37−40.
(52) Nordstrom, D. K. Mine Waters: Acidic to Circumneutral. *Elements* **2011**, *7*, 393−398.
(53) Wang, S. L.; Xu, X. R.; Sun, Y. X.; Liu, J. L.; Li, H. B. Heavy metal pollution in coastal areas of South China: A review. *Mar. Pollut. Bull.* **2013**, *76*, 7−15.
(54) Landrigan, P. J.; Stegeman, J. J.; Fleming, L. E.; Allemand, D.; Anderson, D. M.; Backer, L. C.; Brucker-Davis, F.; Chevalier, N.; Corra, L.; Czerucka, D.; Bottein, M. Y. D.; Demeneix, B.; Depledge, M.; Deheyn, D. D.; Dorman, C. J.; Fénichel, P.; Fisher, S.; Gaill, F.; Galgani, F.; Gaze, W. H.; Giuliano, L.; Grandjean, P.; Hahn, M. E.; Hamdoun, A.; Hess, P.; Judson, B.; Laborde, A.; McGlade, J.; Mu, J.; Mustapha, A.; Neira, M.; Noble, R. T.; Pedrotti, M. L.; Reddy, C.; Rocklöv, J.; Scharler, U. M.; Shanmugam, H.; Taghian, G.; van de Water, J.; Vezzulli, L.; Weihe, P.; Zeka, A.; Raps, H.; Rampal, P. Human Health and Ocean Pollution. *Ann. Global Health* **2020**, *86*, 151 DOI: 10.5334/aogh.2831.
(55) Long, Z. J.; Huang, Y.; Zhang, W.; Shi, Z. L.; Yu, D. M.; Chen, Y.; Liu, C.; Wang, R. Effect of different industrial activities on soil heavy metal pollution, ecological risk, and health risk. *Environ. Monit. Assess.* **2021**, *193*, 1 DOI: 10.1007/s10661-020-08807-z.
(56) Miller, K. A.; Thompson, K. F.; Johnston, P.; Santillo, D. An Overview of Seabed Mining Including the Current State of Development, Environmental Impacts, and Knowledge Gaps. *Front. Mar. Sci.* **2018**, *4*, 418.
(57) Gwyther, D. *Environmental IMPACT statement, Solwara 1 project Main Report Coffey Natural Systems (2008).*; Nautilus Minerals Niugini Limited, Main Report Coffey Natural Systems, 2008.
(58) Fallon, E. K.; Petersen, S.; Brooker, R. A.; Scott, T. B. Oxidative dissolution of hydrothermal mixed-sulphide ore: An assessment of current knowledge in relation to seafloor massive sulphide mining. *Ore Geol. Rev.* **2017**, *86*, 309−337.
(59) Bilenker, L. D.; Romano, G. Y.; McKibben, M. A. Kinetics of sulfide mineral oxidation in seawater: Implications for acid generation during in situ mining of seafloor hydrothermal vent deposits. *Appl. Geochem.* **2016**, *75*, 20−31.
(60) Angel, B. M.; Simpson, S. L.; Jarolimek, C. V.; Jung, R.; Waworuntu, J.; Batterham, G. Trace metals associated with deep-sea tailings placement at the Batu Hijau copper−gold mine, Sumbawa, Indonesia. *Mar. Pollut. Bull.* **2013**, *73*, 306−313.
(61) Brand, L. E.; Sunda, W. G.; Guillard, R. R. L. Reduction of marine phytoplankton reproduction rates by copper and cadmium. *J. Exp. Mar. Biol. Ecol.* **1986**, *96*, 225−250.
(62) Morel, F. M. M.; Price, N. M. The Biogeochemical Cycles of Trace Metals in the Oceans. *Science* **2003**, *300*, 944−947.
(63) Doney, C.; Fabry, J.; Feely, A.; Kleypas, A. Ocean acidification: The other CO_2 problem. *Annual Review of Marine Science* **2009**, *1*, 169−192.
(64) Fouquet, Y.; Cambon, P.; Etoubleau, J.; Charlou, J. L.; OndréAs, H.; Barriga, F. J. A. S.; Cherkashov, G.; Semkova, T.; Poroshina, I.; Bohn, M.; Donval, J. P.; Henry, K.; Murphy, P.; Rouxel, O. Geodiversity of Hydrothermal Processes Along the Mid-Atlantic Ridge and Ultramafic-Hosted Mineralization: a New Type Of Oceanic Cu-Zn-Co-Au Volcanogenic Massive Sulfide Deposit. *Diversity Of Hydrothermal Systems On Slow Spreading Ocean Ridges* **2010**, 321−367, DOI: 10.2113/econgeo.107.2.381.
(65) Bruland, K. W. Trace elements in seawater. *Chem. Oceanogr.* **1983**, *8*, 157−220.
(66) Payne, C. D.; Price, N. M. Effects of cadmium toxicity on growth and elemental composition of marine phytoplankton. *J. Phycol.* **1999**, *35*, 293−302.
(67) Zhou, G.; Luo, J.; Liu, C.; Chu, L.; Crittenden, J. Efficient heavy metal removal from industrial melting effluent using fixed-bed process based on porous hydrogel adsorbents. *Water Res.* **2018**, *131*, 246−254.
(68) Byrne, R. H.; Laurie, S. H. Influence of Pressure on Chemical Equilibria in Aqueous Systems - with Particular Reference to Seawater. *Pure Appl. Chem.* **1999**, *71*, 871−890.
(69) Rainbow, P. S.; Luoma, S. N. Metal toxicity, uptake and bioaccumulation in aquatic invertebrates—Modelling zinc in crustaceans. *Aquat. Toxicol.* **2011**, *105*, 455−465.
(70) Campana, O.; Simpson, S. L.; Spadaro, D. A.; Blasco, J. Sub-Lethal Effects of Copper to Benthic Invertebrates Explained by Sediment Properties and Dietary Exposure. *Environ. Sci. Technol.* **2012**, *46*, 6835−6842.
(71) Lee, J. H.; Birch, G. F.; Cresswell, T.; Johansen, M. P.; Adams, M. S.; Simpson, S. L. Dietary ingestion of fine sediments and microalgae represent the dominant route of exposure and metal accumulation for Sydney rock oyster (Saccostrea glomerata): A biokinetic model for zinc. *Aquat. Toxicol.* **2015**, *167*, 46−54.